Radial distribution of molecular ions in the positive column of dc glow discharges using infrared diode-laser spectroscopy

Fu-shih Pan and Takeshi Oka
Department of Chemistry and Department of Astronomy and Astrophysics, The University of Chicago, Chicago, Illinois 60637
(Received 29 December 1986)

The highly sensitive technique of infrared ion spectroscopy using frequency-tunable diode lasers has been introduced to study radial distribution of molecular ions in the positive column of dc glow discharges. Compared with previous techniques of plasma diagnostics, this method has the advantage that it is *in situ* and nonintrusive, has a high spatial resolution, and is sensitive to quantum states and velocities of molecular ions. ArH^+ in Ar or He discharge and H_3^+ in an H_2 discharge have been used because of the strong infrared absorption and relative simplicity of the plasma chemistry. Our observations show that, while under certain discharge conditions where the radial distribution of molecular ions has the form of the zeroth-order Bessel function $J_0(\sqrt{a/D}\,r)$ predicted by Schottky, it deviates markedly from the Schottky form in most plasma conditions. In particular, for ArH^+ in an Ar plasma under high-current (1.25-A), high-pressure (10-torr) conditions, a large center depletion of the ion is noticed in the observed radial intensity variation of the absorption line. The observed intensity variation has been converted to radial concentration using vibrational and kinetic temperatures determined from relative intensities and widths of spectral lines. The result shows a large center depletion in molecular-ion concentration. Possible causes of such an effect are discussed. The variation of molecular-ion density at the center of the positive column as a function of discharge current has also been measured for ArH^+ and H_3^+.

I. INTRODUCTION

Although gaseous discharges have been known for centuries,[1] our understanding of this physical system is still rather limited. This is due to the complicated interplay of many macroscopic and microscopic physical and chemical processes that occur in the discharge. Theoreticians have found that a complicated mathematical formalism is necessary to describe the system even to a rudimentary extent (see, for example, papers in Ref. 2). Most detailed model studies of gaseous glow discharges are thus limited to the simplest cases of inert gas discharges with relatively low-current density.

In molecular discharges, the chemical composition of the medium is much more complicated. The efficient ion-molecule reactions which have a large Langevin rate (typically 10^{-9} cm^3/sec) produce and destroy ions rapidly. The rich internal structure of molecules also introduces additional processes, such as dissociative recombinations, which can play significant roles in the system. For example, the rate constants of the dissociative recombination of molecular ions are 10^4–10^7 times larger than those for atomic ions. Furthermore, the rates of many processes depend on the internal state of molecules.

Traditionally a Langmuir probe or a mass spectrometer have been used to study plasma. These methods inevitably perturb the plasma and thus cannot monitor the interior of the plasma. Optical spectroscopic methods do not have these drawbacks but have been mostly used only for monitoring neutral species, since charged species usually do not emit or absorb optical radiation efficiently. Thus, little information is available for diagnostics of molecular ions *in situ* in plasmas. Some new experimental method is highly desirable for a better understanding of molecular discharges.

In the past several years molecular-ion spectroscopists have been very successful in observing and analyzing novel *infrared* spectra of molecular ions using laser spectroscopic techniques and discharges.[3,4] Such spectroscopy provides us with a novel experimental tool for plasma diagnostics. Although the method is not as sensitive as the mass spectroscopic method and its application is limited to molecular ions with relatively high density ($\gtrsim 10^8$ cm^{-3}), it has the following advantages over the traditional methods.

(1) The method is *in situ* and nonintrusive because of the weak interaction between the radiation and the plasma medium. We can probe any part of the plasma without significantly perturbing it.

(2) The method has good spatial resolution since the laser beam can be well collimated and small in diameter ($4\sim 6$ mm).

(3) The method allows us to monitor molecular ions in individual quantum states. For example, we can obtain vibrational and rotational temperatures of the plasma from relative intensities of spectral lines.

(4) The Doppler shifts and the widths of spectral lines provide information on the drift velocities and the random velocities of molecular ions, respectively, thus allowing us to determine the ion mobility and translational

temperature of ions. These advantages were used in our earlier paper on the measurement of mobility of ArH^+ in He buffer.[5] In this paper we apply laser infrared spectroscopic techniques to the study of ion density distributions across the positive columns of dc glow discharges.

The distribution of ions in plasma was first studied theoretically by Schottky[6] in 1924. Schottky proposed the ambipolar diffusion mechanism and predicted that the radial ion-density distribution in a cylindrical positive column takes the form of the zeroth-order Bessel function $J_0(\alpha r)$. The assumptions employed in the theory are one step ionization, quasineutrality, constant temperature, and others which make the theory applicable only to low-current discharges of inert gases.[7] Many attempts to extend Schottky's theory have been reported for discharges with higher current densities and pressure by including stepwise ionization,[8] recombination,[9] and lifting the assumption of constant temperature.[10] Under certain discharge conditions the extended theory of Ecker and Zoller[10] predicted considerable deviations from Schottky's form. Lindinger[11] has reported "non-Schottky" ion distributions in his hollow cathode discharge using mass spectroscopic methods. However, Schottky's original prediction of Bessel-function shapes has generally been accepted as valid for the positive column of discharges and a few available experimental results seem to confirm this.[12]

In this paper we apply the laser infrared spectroscopic method to study the ion distribution *in situ* in discharges. We use relatively simple H_2 and Ar-H_2 discharges and strong absorption lines of H_3^+ (Ref. 13) and ArH^+ (Ref. 14) in the 4-μm region. We observed Schottky's form in certain cases but also marked deviations from it under certain discharge conditions. Especially for the ArH^+ ion in Ar-dominated discharges, a pronounced minimum of ion density was observed at the center of the positive column. The observation and some qualitative interpretation will be given in this paper. We also discuss current dependence of ion densities in discharges. Other applications of laser spectroscopic techniques–for plasma diagnostics have been reported.[15–17]

II. H_3^+ AND ArH^+

The hydrogen discharge is the simplest of molecular discharges and its study is the first step towards the understanding of molecular discharges. The kinetic temperature of electrons in the positive column of a glow discharge is typically a few electron volts. The primary ionization of H_2 (ionization energy 15.4 eV),

$$H_2 + e^- \rightarrow H_2^+ + e^- + e^- \quad (1)$$

is, therefore, effected by the tail of the kinetic-energy distribution of electrons. The H_2^+ ion thus produced immediately reacts with H_2 to produce the H_3^+ ion through the efficient ion-molecule reaction,

$$H_2^+ + H_2 \rightarrow H_3^+ + H \quad (2)$$

which is exothermic by 1.8 eV and has a Langevin rate (see Ref. 18 for a summary of work on H_3^+). The H_3^+ ion is destroyed either by the electron recombination reactions[19] or collisions with the wall after ambipolar diffusion. Since these destruction rates of H_3^+ are smaller than the ion-molecule reaction rate of Eq. (2), H_3^+ is the dominant ion in the hydrogen discharge. The production of the cluster ion H_5^+ through the three-body association reaction,[20]

$$H_3^+ + H_2 + H_2 \rightarrow H_5^+ + H_2 \quad (3)$$

is not expected to affect the dominance of H_3^+ in our discharge conditions. The strong ν_2 fundamental vibration rotation band[13] of H_3^+ [transition dipole moment 0.156 Debye (Ref.21)] provides an excellent means to probe this ion. We use the $^RQ(1,0)$ transition at 2529.724 cm^{-1}; this choice is partly because of its large intensity and partly because of the convenience of operating the diode laser in the 4-μm region.

The ArH^+ ion produced in an Ar discharge with a trace of H_2 was the most convenient probe for plasma diagnosis partly because of the simplicity of the discharge but more so because of its large absorption intensity. In an Ar discharge, both the electric field and the electron drift velocity are low and thus a larger number of charged species exist for the same current density. From the observed intensities of the ArH^+ spectral lines, we estimate the number density of ArH^+ to be on the order of 10^{12} cm^{-3}. This large concentration together with its large transition dipole moment of 0.25 Debye (Ref. 22) and the large rotational constant of 10.46 cm^{-1} (Ref. 14) make this ion the strongest infrared absorber of all molecular ions. The strength of the absorption not only makes the measurement easy and accurate but also allows us (a) to use the simple video detection technique which gives us the intensity, width, and line shape without distortion and (b) to observe the vibrational hot band $v=2\leftarrow1$ to determine vibrational temperature and the vibrational dependence of the radial ion distribution. The production and destruction of ArH^+ is similar to that of H_3^+ given above except that the ion-molecule reaction is

$$Ar + H_2^+ \rightarrow ArH^+ + H \quad (4)$$

or

$$Ar^+ + H_2 \rightarrow ArH^+ + H \quad (5)$$

both of which have the Langevin rate and are exothermic (1.2 and 1.6 eV, respectively). Out of the great many spectral lines, reported by Brault and Davis,[14] we choose as our probe the $P(3)$ transition of the fundamental band $v=1\leftarrow0$ at 2525.475 cm^{-1} and the $R(2)$ transition of the first hot band $v=2\leftarrow1$ at 2525.414 cm^{-1}. It is convenient that they appear close in frequency so that information for $v=0$ and 1 ArH^+ can be obtained simultaneously.

III. EXPERIMENTAL

The simple setup used for the measurement of the radial ion-density distribution is shown in Fig. 1. This design is identical to that by Bleekrode and Laarse[23] except that we use an infrared laser and monitor ions directly. The infrared radiation was generated from the LS-3 infrared

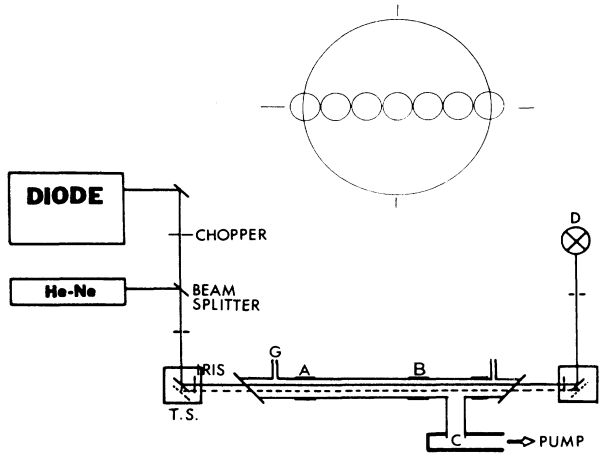

FIG. 1. Basic setup for the experiment. The infrared laser beam from the frequency-tunable diode was passed through the discharge tube. The radial position of the beam was adjusted by moving two mirrors which were mounted on the translation stages (T.S.) before and after the discharge tube. The two irises mounted on the same translation stages minimized the laser beam diameter to 4 mm for higher spatial resolution. The cross section of the discharge tube is given in the inset with the laser beam diameter indicated. Because of the Gaussian power profile of the laser beam intensity, the effective beam diameter is smaller than 4 mm, the spatial resolution is $2R/d_{\text{eff}} \gtrsim 10$. G, gas inlet; A, anode; B, metal connector for voltage measurement; C, cathode; D, detector.

diode laser system of spectra physics. We chose the appropriate mode of the laser oscillation using the monochromator of the system but skipped the monochromator when we did spectroscopy. This allowed us to have more intense infrared laser radiation with better alignment and a smaller beam diameter to increase the spatial resolution. The infrared radiation was collimated with the radiation from a HeNe laser for the alignment and manipulation of the beam.

The accurate alignment and shift of the laser beam were done using irises and two mirrors each mounted on a translation stage. First the beam was collimated with the center of the discharge tube using irises placed inside the tube. Then the horizontal beam position was adjusted by moving the two horizontal stages. The diameter of irises mounted on the translational stage were minimized in order to have a maximum spatial resolution. They were 4 mm for the ArH^+ experiments and 6 mm for the H_3^+ experiment; the H_3^+ lines were weaker and we could not afford to lose laser power by closing the iris further. The inner diameter of the discharge cell was 21 mm and the cross section of the tube is shown in the inset of Fig. 1 with the laser beam diameter indicated for the case of the ArH^+ experiment. Since the laser power profile is Gaussian, we estimate our spatial resolution to be ~ 10. For experiments using an air-cooled discharge tube we could cover about 90% of the radial position, while for those using a liquid-nitrogen-cooled discharge tube the coverage was less and $\sim 80\%$.

Two discharge tubes, one air-cooled and the other liquid-N_2-cooled, were used for the experiment; they both had lengths of 2 m and an inner diameter of 21 mm. A water-cooled cathode (C in Fig. 1) which allows a high current (1.25 A) was attached to a side arm of the discharge tube so that the cathode discharge region was out of the radiation path and thus only ions in the positive column were probed. The anode A was a Cajon joint which also connected the main tube and the Brewster angle section. An additional Cajon joint B, which connected the main tube and the T section for the cathode, was used to measure the electric potential of the plasma for estimating the field strength in the positive column. The cathode potential drop estimated from the voltage difference between B and C agreed approximately with values reported in the literature.[24] The dc power supply for the discharge was current regulated and generated voltages up to 50 kV and current to 1.25 A. Pressure of the gas was measured using an MKS capacitance manometer. The discharge tube was sealed with two CaF_2 Brewster-angle windows.

For the ArH^+ experiment the H_2 pressure was kept at 30 mTorr and argon was added to the total pressure of 1–10 Torr. For the H_3^+ experiment, a liquid-nitrogen-cooled H_2 discharge at a pressure of 0.55–1.15 Torr was used. The kinetic temperature of gas was 200 K (Refs. 25 and 26) and the gas density was higher than that in the air-cooled cell by a factor of $3\sim4$ for the same pressure. The discharge conditions for observation were limited by the requirement of stable discharges. From the observed voltage-current characteristics and the appearance of cathode glow, we believe that under some high-current conditions, the discharge was in the region of glow to arc transition, i.e., the abnormal discharge.[12]

Two modes of detection were used for observing the spectral lines. The video detection, in which the laser beam was chopped and amplified at the frequency of the chopper, was less sensitive but gave more reliable quantitative information on the intensity, width, and shape of spectral lines. This method was used for ArH^+ lines but could not be used effectively for the weaker H_3^+ line. We used the method of frequency modulation and $2f$ detection as the second detection method. This method is much more sensitive and allowed easier detection with less time constant and time of observation, although often quantitative information on absolute magnitude was difficult to elucidate. Since most of our measurements are for relative magnitude the latter method was used more than the former. One complication arises from the variation of laser power depending on frequency of laser and the time of measurement. Therefore, we always measured the laser power and took relative value of the absorption signal to the laser power.

IV. OBSERVED RESULTS

A. Deviation from the Schottky form

It did not take long to find the variation of line intensities across the discharge tube does not follow the simple zeroth-order Bessel function as expected from Schottky's

theory. Our observation will be summarized below for individual spectra lines.

1. *The fundamental $v=1\leftarrow 0$ $P(3)$ line of* ArH^+

The observed variations of absorption intensities for the $P(3)$ line in the fundamental band of ArH^+ are shown in Figs. 2–5 for various discharge conditions. The intensities of the signal are normalized such that the intensity at the center of the discharge tube is unity.

For the case of relatively low total pressure of 1 Torr (with 30 mTorr of H_2) and low current of 300 mA, shown in Fig. 2, the observed shape is very close to the Schottky's curve (shown in the figure with a solid line). We believe that the small deviation from the curve near the wall was due to the finite size of the laser beam. However, a recent calculation of Ernie and Oskam[27] shows that such behavior in the positive column arises from a space-charge effect. Figure 3 shows our results for the same $Ar:H_2$ mixture but with differing discharge current. The case of the lowest current (250 mA) shown with open circles is the same as for Fig. 2. As the current increases from 750 mA (closed circles) to 1250 mA (triangles) the curve deviates from the Schottky form indicating a relatively higher concentration of ArH^+ in the noncentral area.

When the pressure of the discharge gas is increased, the deviation from Schottky's form becomes more pronounced. Observed results for the total pressure of 6 Torr (the partial pressure of H_2 is still kept at 30 mTorr) are shown in Fig. 4 for different currents. For the lowest current of 250 mA (open circles) the curve is slightly de-

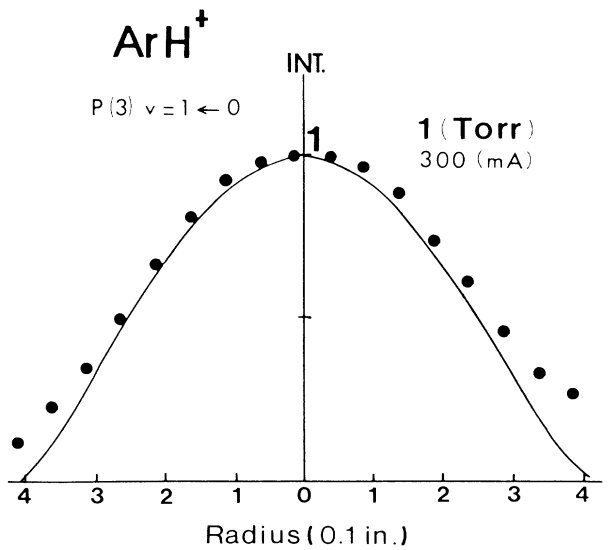

FIG. 2. The spectral intensity profile across the discharge tube for the fundamental line of ArH^+ from the discharge of $Ar:H_2=30:1$ mixture. The total pressure of the discharge is 1 Torr and discharge current 300 mA. Observed intensity profiles shown with filled circles are normalized to the center. The curve indicates the calculated Schottky form. In this discharge condition, the observed result is very close to the Schottky form.

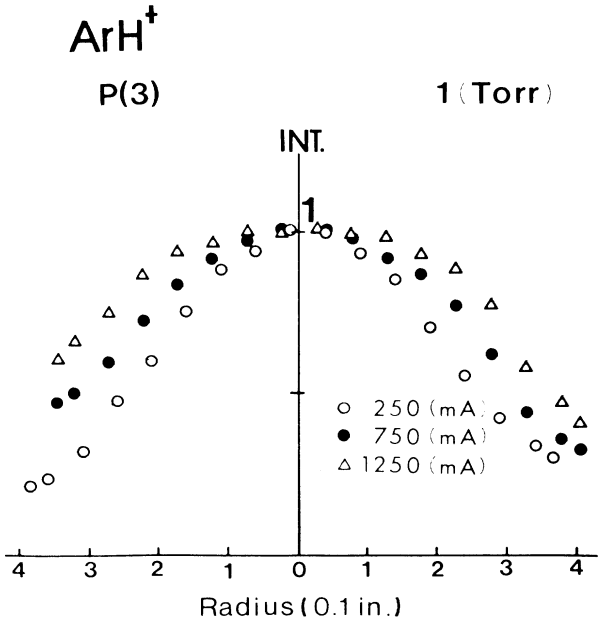

FIG. 3. The same result as shown in Fig. 2 but for varying discharge currents, 250 mA (○), 750 mA (●), and 1250 mA (△). The observed profile deviates from the Schottky form as the current is increased.

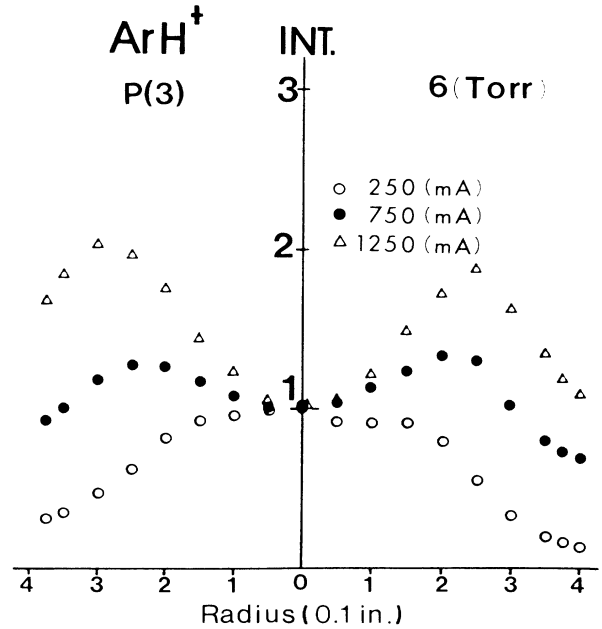

FIG. 4. The observed intensity profiles for the ArH^+ fundamental $P(3)$ line for higher pressure of 6 Torr (the partial pressure of the H_2 was kept constant and the mixing ratio now is $Ar:H_2=250:1$) and various currents, 250 mA (○), 750 mA (●), and 1250 mA (△). A marked deviation from the Schottky form is noticed for higher-current discharges. Clear center depletion is observed for 6 Torr and 1250 mA discharge.

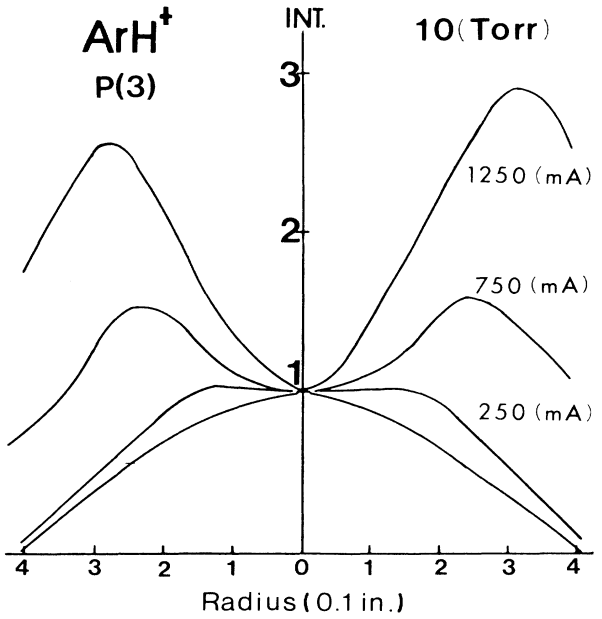

FIG. 5. The same result as shown in Fig. 4 with higher total pressure of 10 Torr. ($Ar:H_2=330:1$). The center depletion is even more pronounced. The maximum of the spectral intensity is found to be closer to the wall for a higher current.

formed from Shottky's form, but for the higher discharge current of 750 mA (closed circles), a clear minimum of the signal intensity was observed at the center of the discharge tube and the intensity of the line at maximum, which occurs approximately at the midpoint between the center and the wall, and was about 30% higher than that at the center. This deviation from the Schottky form becomes larger for the higher discharge current of 1250 mA (triangles) for which the ion signal at the center of the tube was about one-half of that at the maximum, and the maximum occurred even closer to the wall. The effect was observed to be even more pronounced if we went to higher pressure. The results for the pressure of 10 Torr are shown in Fig. 5 again for the three discharge currents. For the highest pressure-current combination of 10 Torr and 1250 mA, the maximum to minimum intensity ratio is nearly 3. The apparent asymmetry of the curve for this case may be due to small distortion of the discharge tube but may also be due to transition to an arc discharge. We see the glow more constricted and slightly distorted under high-pressure high-current conditions.

The raw observed signals for the discharge of 10 Torr and 1250 mA are shown in Fig. 6, to demonstrate the high signal-to-noise ratio of the ArH^+ absorption lines recorded by the frequency modulation ($2f$ detection) with only 2 m of optical path and the remarkable center depletion of the ArH^+ ions.

2. *The hot band $v=2\leftarrow 1$ R(2) line of* ArH^+

The variation of the intensity of the hot-band transition across the discharge tube was observed to be consid-

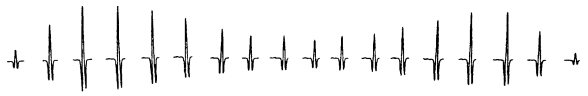

FIG. 6. The raw spectroscopic data showing the center depletion. The absorption line is the $P(3)$ transition of ArH^+ fundamental band. The detection of the spectra was made by frequency modulation and $2f$ detection. The signal-to-noise ratio is typically 100. The spatial separation between adjacent signals is approximately 1 mm.

erably different from that of the fundamental band because the number of ArH^+ ions in the $v=1$ vibrational state ($2710\ cm^{-1}=3900$ K above the ground state) is highly sensitive to temperature which is a function of the radial position of the discharge tube. The variation of the hot-band line is compared with that of the fundamental line in Figs. 7 and 8 for two pressure-current conditions under which the fundamental line deviates significantly from the Schottky curve. Compared with the profile for the fundamental band, the hot-band profile is much more concentrated to the center because of the high temperature at the center and low temperature towards the wall.

It is seen in Fig. 7 for the discharge of 1 Torr and 1250 mA, that the fundamental profile is considerably wider than the Schottky form but that the hot-band profile is narrower. For the discharge of 6 Torr and 1250 mA

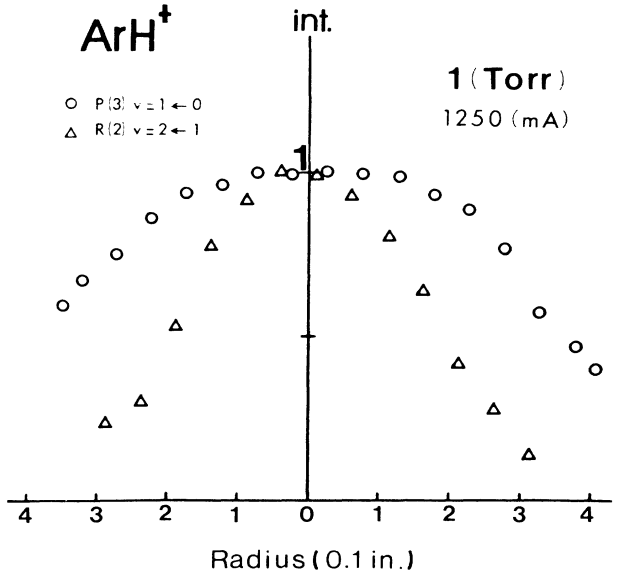

FIG. 7. Comparison of intensity profile across the discharge tube for the $P(3)$ fundamental band and the $R(2)$ hot band of ArH^+. The hot-band transition (△) is much weaker but is normalized to the fundamental (○) at the center of the discharge tube. It is noticed that the hot band tails off much quicker when the laser probe is moved close to the wall because of the temperature effect. Vibrational temperature across the tube can be determined from this type of observation.

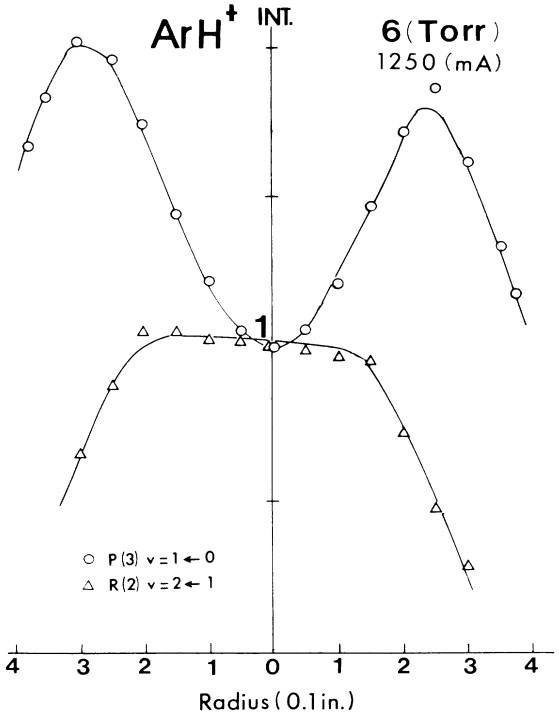

FIG. 8. Intensity profile across the discharge tube for the hot-band $R(2)$ transition (△) and the fundamental band $P(3)$ transition (○) for high total pressure (6 Torr) and high-current (1250 mA) discharge. The difference between the two profiles is more pronounced for this discharge condition.

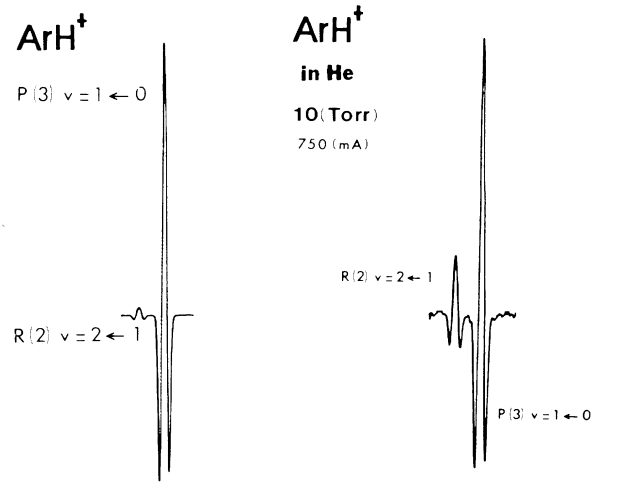

FIG. 9. Typical spectral scans for the ArH^+ ion in Ar discharge and that in He. The stronger line is the fundamental $P(3)$ transition while the weaker line is the hot-band $R(2)$ transition. The relative intensity of the hot-band line is increased greatly in the He discharge indicating much higher vibrational temperature in the He discharge.

shown in Fig. 8 where the clear center minimum was observed for the fundamental line, the hot-band profile is still reasonably close to the Schottky form although the flattening at the center and the rapid falloff to the wall are clearly noticed. The ratios of the intensities for the fundamental line and the hot-band line give the variation of vibrational temperatures across the discharge tube. This will be discussed later in Sec. V A.

3. ArH^+ *in* He *discharge*

When the ArH^+ ion was produced in a plasma in which He was the dominant component, the characteristics of the plasma changed drastically. For this experiment we used a gas mixture of $[H_2]$:Ar:He $\sim 3.20:1000$ with the total pressure of ~ 10 Torr. The use of He increased the vibrational temperature, the translational temperature, and the mobility of the ArH^+ ion. The large increase in vibrational temperature is clearly seen from Fig. 9 in which traces for the $v=1\leftarrow 0$ $P(3)$ line and the $v=2\leftarrow 1$ $R(2)$ line are shown for the two cases of Ar-dominated discharge and for the He-dominated discharge. The large increase in the relative intensity of the weaker line shows that the vibrational temperature increased from 900 to 2200 K in going from Ar discharge to He discharge.

The radial intensity variation of the ArH^+ ion was also observed to be quite different in the He discharge from that in the Ar discharge. Our results for a high-pressure current of 10 Torr and 750 mA are given in Fig. 10 for both the fundamental and the hot band transitions. Compared with the case of Ar discharge shown in Fig. 5, the center depletion is very slight if any and the distribution of the ion is much more uniform across the tube. The variation of vibrational temperature also seems to be less across the tube.

4. H_3^+ *in* H_2 *discharge*

The radial intensity variation of the H_3^+ absorption line was observed to be very similar to that of ArH^+ in the He discharge. Because of the smaller intensity of the H_3^+ line, the measurement of the variation was limited to the discharge condition of 550 mTorr and 250 mA which gave the strongest absorption line. The results of our measurement are shown in Fig. 11. It is noticed that the line intensity is almost constant across the discharge tube.

B. Variation of the absorption with discharge current

So far we have reported the observed variation of relative intensities of spectral lines normalized to the observed value at the center for each discharge condition. In this section we summarize our observed results of the variation of the center intensity as a function of discharge current.

1. ArH^+

The observed dependence of the $v=1\leftarrow 0$ $P(3)$ ArH^+ absorption line on the discharge current for various discharge pressures is shown in Fig. 12. The variation is rather complicated. At the low total pressure of 1 Torr,

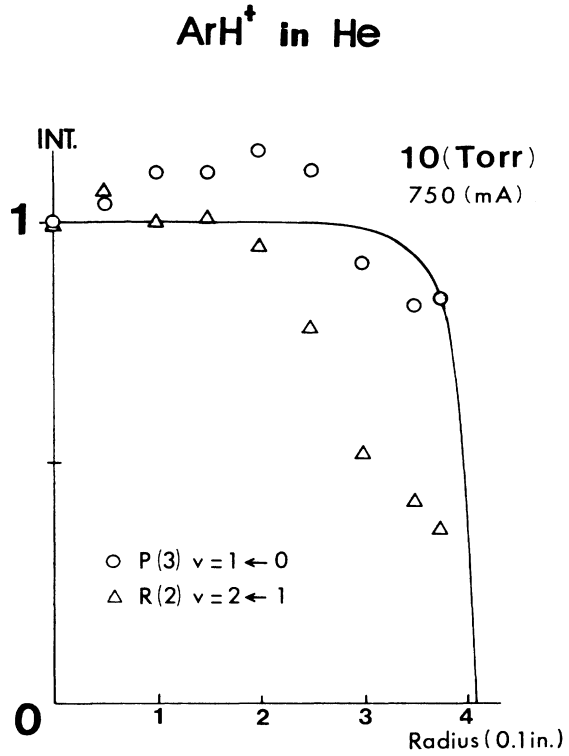

FIG. 10. Variation of spectral intensity across the tube for the fundamental (○) and hot-band (△) transition from the high-pressure (10 Torr) high-current (750 mA) case of ArH^+-He discharge. The profile is qualitatively different from the case in the Ar discharge (Fig. 5).

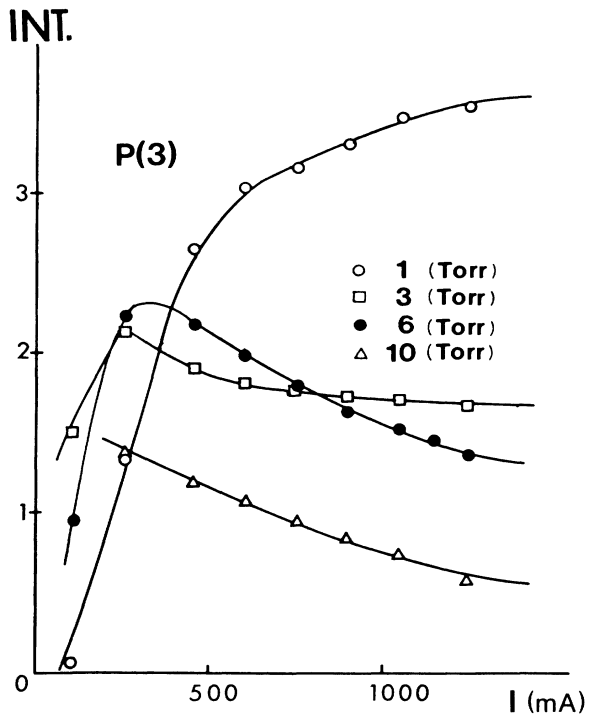

FIG. 12. Variation of ArH^+ fundamental $P(3)$ spectral intensity at the center of the discharge tube as a function of the discharge current for the total pressure of 1 Torr (○), 3 Torr (□), 6 Torr, (●), and 10 Torr (△). The decrease of signal intensity for high-pressure cases is due to center depletion.

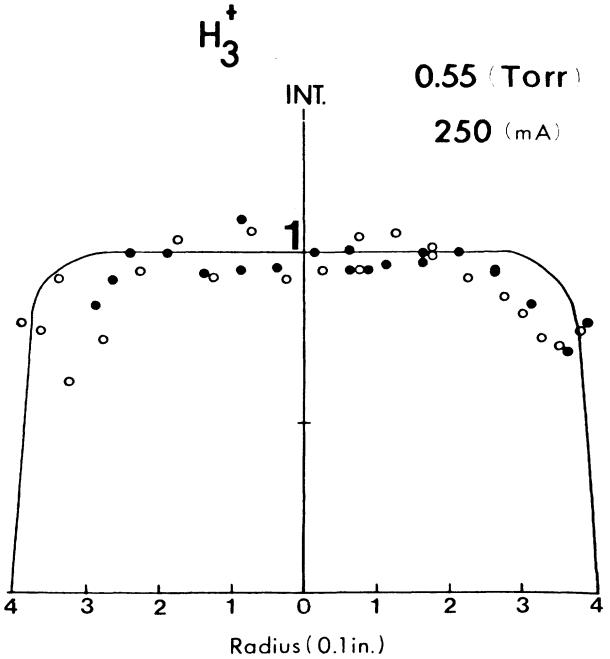

FIG. 11. Spectral intensity variation across the discharge tube for H_3^+. The profile is very different from that of ArH^+ given earlier and deviates from the Schottky form even under low-pressure–low-current conditions.

the line intensity increases with the current although the increase is slower at higher current. For a pressure at 3 Torr or higher, the line intensity increases with the pressure initially, reaches the maximum at relatively low current, and then decreases slowly with the current. For the whole experiment the hydrogen partial pressure was kept constant. The measurement was done mostly using the frequency modulation—$2f$ detection but the absolute intensity was calibrated at a few points using video detection. One example of the video detection signal is shown in Fig. 13. This signal shows an absorption of $\sim 17\%$ corresponding to the ArH^+ ion density of $\sim 1\times 10^{12}$ cm^{-3} on the assumption of the rotational temperature of 730 K.

2. H_3^+

The variation of the H_3^+ line intensity at the center of the tube was measured repeatedly as a function of pressure and current. The results of measurements made for the presure of 0.55, 0.7, 0.85, 1.0, and 1.15 Torr are summarized in Fig. 14. The current dependence of the intensity is rather complicated and indicates the difficulty of analyzing molecular plasma even for this simplest case. A particularly puzzling feature is the occurrence of a double maximum for the pressure of 0.7 Torr, which was confirmed by repeated measurements. For the lowest

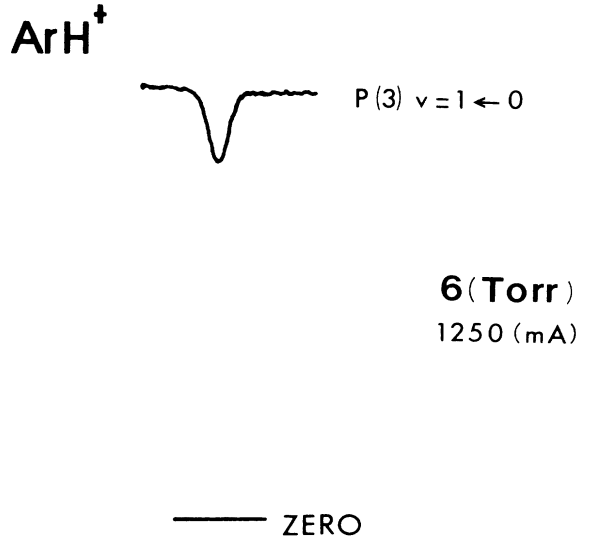

FIG. 13. An example of the ArH^+ fundamental $P(3)$ spectral line observed by video detection. The large absorption (17%) after the path length of only 2 m indicates a large ArH^+ concentration of 1×10^{12} cm^{-3}.

pressure of 0.55 Torr, the line intensity was most critically dependent on the current and showed a fairly sharp maximum. For higher pressures, the current dependence was less.

From these results we note that the maximum signal was obtained at the pressure of 0.55 Torr and the current of 250 mA ($\sim$70 mA/cm^2). At this condition the number density of H_3^+ is estimated to be $\sim7\times10^{11}$ cm^{-3} assuming the rotational temperature to be 200 K.[25,26]

C. Linewidth measurement

Linewidth of the fundamental $P(3)$ transition of ArH^+ was measured to obtain information on the random velocity and thus the kinetic temperature of ArH^+ in the discharge. The Doppler linewidth (HWHM) is related to the kinetic temperature by[28]

$$\Delta\nu_D=\nu_0(2\ln2\,kT/M)^{1/2}/c\ , \tag{6}$$

where ν_0 is the frequency of the absorption line and M is the mass of ArH^+. This value is on the order of 90$\sim$150 MHz for kinetic temperature of 500$\sim$1500 K.

The second cause of linewidth, pressure broadening, can be estimated from

$$\Delta\nu_p=\frac{e(\alpha/\mu)^{1/2}}{kT}\ , \tag{7}$$

where α is the polarizability of the collision partner (Ar) and μ is the reduced mass for ArH^+-Ar. Using the polarizability of the Ar atom of 1.6×10^{-24} cm^3, $\Delta\nu_p$ is calculated to be 2$\sim$0.7 MHz/Torr for the temperature of 500$\sim$1500 K. Thus the Doppler broadening is the dominant factor for the linewidth.

The video detection was used for the measurements of linewidth to avoid complication from modulation. Variation of kinetic temperature was observed across the tube; this will be discussed later in Sec. V B.

V. ANALYSIS

The spectroscopic method gives definitive measurements for each quantum state of molecular ions. However, a careful analysis is needed to obtain information on the total ion density from the observed strength because the conversion from the spectral intensity to the ion density depends critically on the molecular distribution over various quantum states. The absorption coefficient γ (cm^{-1}) at the maximum is related to the total number density n of molecular ions by

$$\gamma=\frac{8\pi^2\nu n}{3hc\,\Delta\nu}\,|\mu_{ij}|^2 f(T_r,T_v)[1-\exp(-h\nu/kT_v)]\ , \tag{8}$$

where ν is the frequency of transition, $\Delta\nu$ is the Doppler width given in Eq. (6), $f(T_r,T_v)$ is the fraction of molecular ions in the lower quantum state of the transition, depending on the vibrational and rotational temperature T_v and T_r, and $|\mu_{ij}|$ is the transition dipole matrix element. The temperatures T_r and T_v can be determined experimentally from relative intensity measurements for different transitions. Rotational temperature was not measured in this experiment and was assumed to be equal to translational temperature due to the fast rotation to translation energy transfer. Because of the intricate dependence of the absorption coefficients on temperatures, a careful analysis is needed to confirm that the observed non-Schottky shape for the line intensities indeed corresponds to that of molecular ion density.

A. Vibrational temperature

The relative intensities of the two ArH^+ lines given in Sec. IV A 2 provide us with vibrational temperature at each radial position of the discharge tube. The relative intensities of the two lines are related to the vibrational temperature T_v by

$$\rho=\frac{I(v=2\leftarrow1,\,R(2))}{I(v=1\leftarrow0,\,P(3))}=C\exp(-\Delta E/kT)\ , \tag{9}$$

where ΔE is the separation of the $v=1$ and 0 vibrational levels, i.e., 2710 cm^{-1}.[14] The proportionality constant C depends on rotational temperature but the dependence is neglected in our analysis because the energy separation between $J=2$ and 3 levels ($\sim$60 cm$^{-1}\sim$100 K) is much smaller than the temperature in the discharge (500$\sim$1500 K). The value of C is about 1.26 from the ratio of the vibrational matrix elements

$$\langle v+1\,|\,q\,|\,v\rangle=\sqrt{(v+1)/2} \tag{10}$$

(which gives 2 as the ratio of the square of the transition moment but this number is more accurately calculated by Rosmus[22] to be 1.86), and the ratio of degeneracy $(2J+1)$. The direction cosine matrix elements of $P(3)$ and $R(2)$ are exactly equal. Equal translational temperature was used for both transitions because their linewidths are equal.

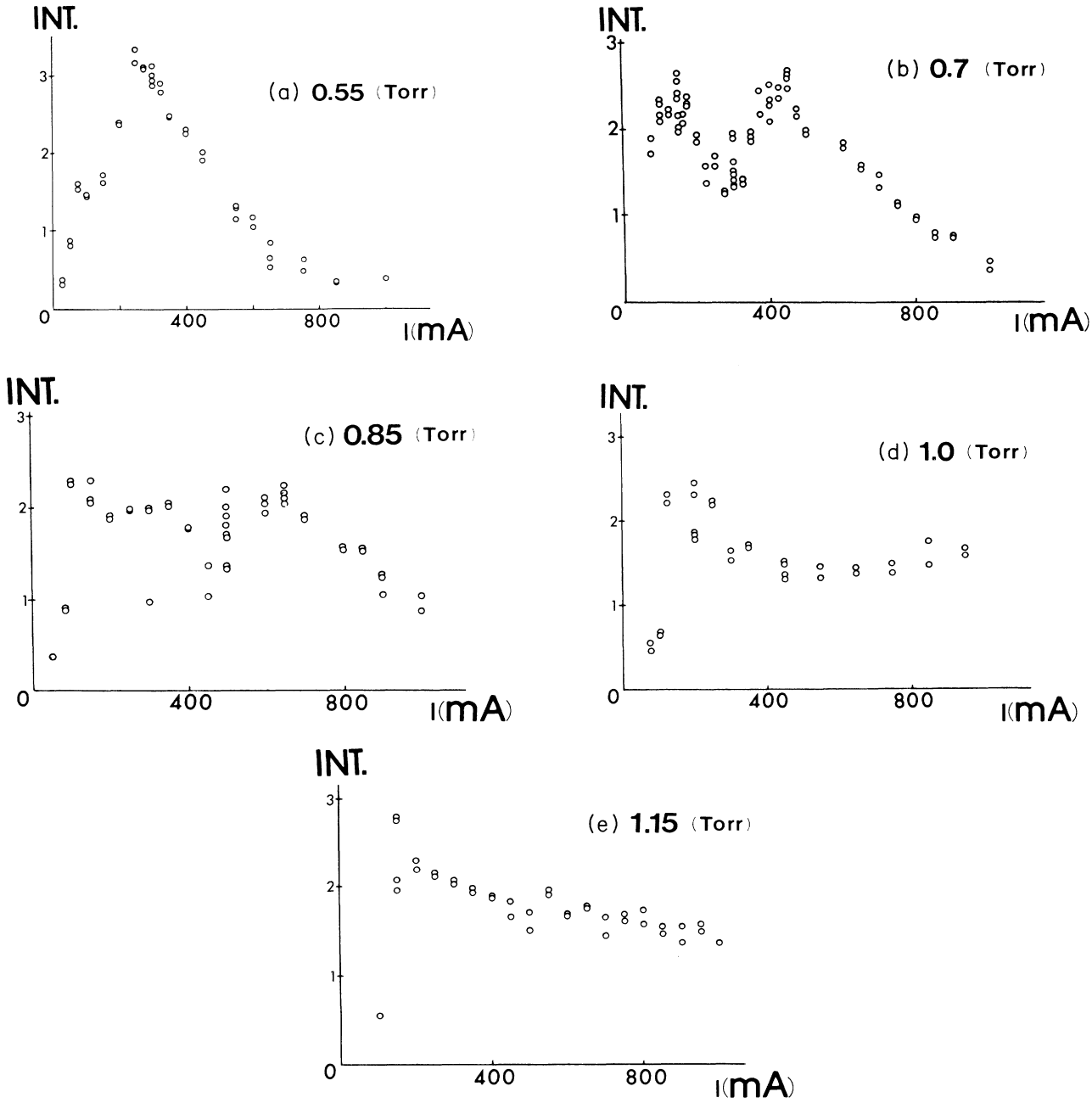

FIG. 14. Variation of H_3^+ spectral intensity at the center of the discharge tube as a function of discharge current at LN_2 temperature for the pressure of 0.55, 0.7, 0.85, 1.0, and 1.15 Torr. The maximum signal was observed for 0.55 Torr and 250 mA. The complicated dependence on the discharge current for the pressure of 0.7 Torr has been confirmed by repeated measurement.

The variation of vibrational temperature across the discharge tube determined from the observed results for ArH^+ in Ar given in Figs. 7 and 8 are shown in Fig. 15. For both pressures of 1 and 6 Torr the vibrational temperature is ~ 1000 K at the center of the discharge tube and falls parabolically to ~ 800 K at the wall of the tube. The higher current gave somewhat higher temperature but the difference is not very large.

The variation of the intensity ratio at the center of the discharge tube with the discharge current, was observed to be as shown in Fig. 16. The ratio is linearly dependent on the current and fits well to the formula

$$\frac{\rho}{C}=\exp\left[-\frac{\Delta E}{kT_v}\right]=\alpha I \tag{11}$$

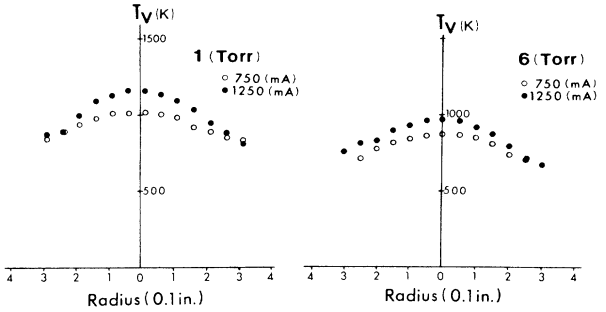

FIG. 15. Variation of vibrational temperature across the discharge tube for various discharge condition. This relatively small variation of T_v across the tube explains the marked difference between the intensity profiles for the fundamental band and the hot band (Figs. 7 and 8).

with $c\alpha=0.04$ A^{-1} for the pressure of 1 Torr and 0.018 A^{-1} for 3, 6, and 10 Torr. The remarkably good fit of the observed intensity ratio to this puzzling relation is not surprising because of the narrow region of temperature variation. If we convert the observed ratio of intensities to T_v we obtain the results plotted in Fig. 17, which fits well to the usual relation

$$T_v=a+bI \ . \tag{12}$$

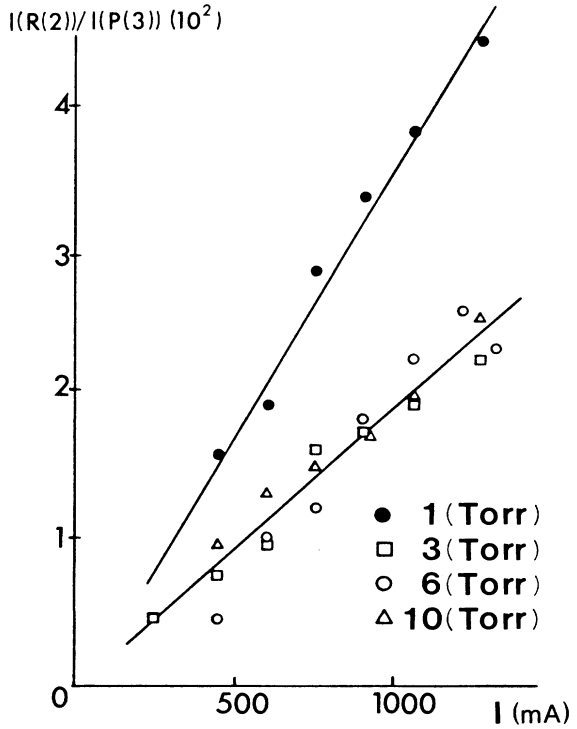

FIG. 16. The variation of intensity ratio of the hot band and the fundamental band as a function of discharge current. See text for explanation.

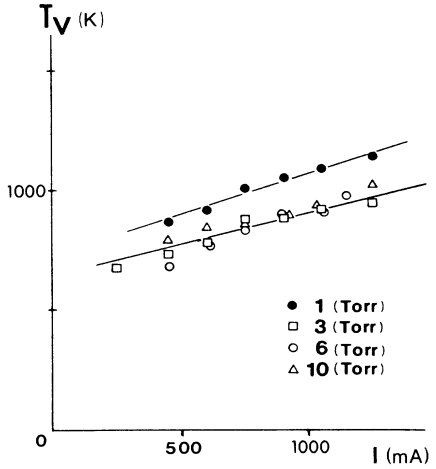

FIG. 17. Dependence of the vibrational temperature on the discharge current determined from the data shown in Fig. 16.

The constants a and b can be related to the constants in Eq. (11) with a good approximation as

$$\begin{aligned} a&=T_0(1-\xi) \ , \\ b&=\alpha T_0\xi\exp(1/\xi) \ , \end{aligned} \tag{13}$$

where $\xi=kT_0/\Delta E$ and T_0 is the hypothetical zero-current temperature.

One remarkable feature of the results shown in Fig. 16 is the large difference in the values of ρ between the pressure of 1 Torr and other higher pressures. The same phenomenon was also observed for the variation of ion density shown in Fig. 12 and discussed later. This suggests a qualitative change of plasma properties between 1 Torr and 3–10 Torr.

The vibrational temperature of ArH^+ in the He discharge is on the order of 2500 K, as determined from the results given in Fig. 9. This is higher than the temperature in the Ar discharge by a factor of ~ 2.5. More recently, ArH^+ in He was studied in an AC discharge at several kHz; in such discharges the vibrational temperature was observed to be even higher by another factor of 2–5 due to the slow vibrational relaxation.[29]

B. Kinetic temperature

The linewidth measurements given in Sec. IV C provide the translational temperature of ArH^+ in the Ar discharge according to Eq. (6). Rotational temperature was not measured in this work and is assumed to be equal to the translational temperature because of the rapid rotation-translation relaxation. The kinetic temperature determined from the linewidth measurement is plotted in Fig. 18 together with the vibrational temperature for various pressures as a function of the discharge current. It is noted that the two temperatures are approximately equal in these discharges. The variation of kinetic temperature across the discharge tube was also similar to that of vibrational temperature. These are in

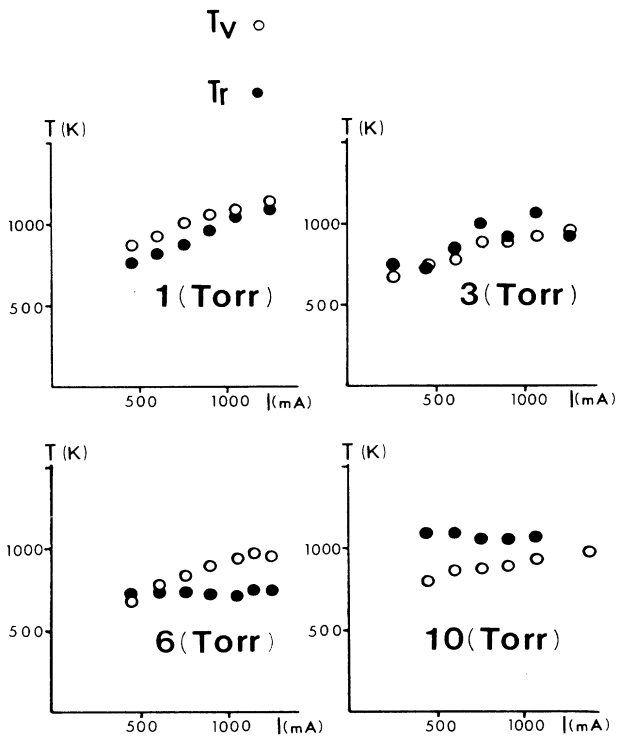

FIG. 18. Dependence of the rotational (●) and vibrational temperatures (○) on the discharge current at the center of tube for different pressures. The two temperatures vary similarly for different conditions.

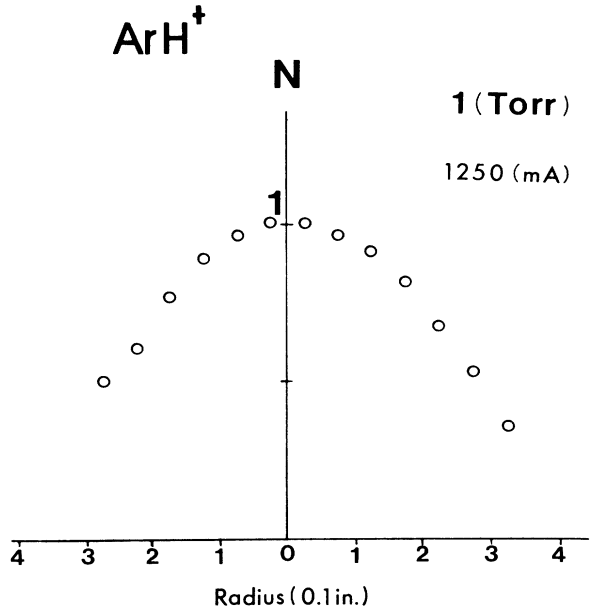

FIG. 19. The ion number density profile of ArH^+ obtained from the observed intensity profile after the temperature correction. The 1 Torr and 1250 mA data plotted in Fig. 3 were used as the intensity profile and the temperature correction was made based on the temperature profile given in Fig. 15. Although the original intensity profile deviates from Schottky form, the ion-density profile is close to the Schottky form after the temperature correction.

contrast to the case of ArH^+ in He discharge where vibrational temperature is much higher than the kinetic temperature. The vibrational relaxation of ArH^+ must be much faster in Ar than in He. This is partly due to the faster V-T transfer in the ArH^+-Ar system but probably due more to the vibrational cooling produced by the proton transfer reaction

$$ArH^+ + \tilde{A}r \rightarrow Ar + \tilde{A}rH^+ \quad (14)$$

which occurs with the Langevin rate.

C. Ion density

The information on various temperatures given above allows us to calculate the ion-density variation across the discharge tube. The result for a low pressure 1 Torr and high current of 1.25 A is shown in Fig. 19. This curve agrees well with the Schottky form in spite of the fact that the raw line intensity curve shown in Fig. 3 is somewhat flatter than the Schottky curve. Thus the deviation from the Schottky form in this case seems to be explained by the effect of temperature variation on the intensities of the spectral line. We therefore studied carefully the temperature effect on the high pressure-current cases shown in Figs. 4 and 5 which showed the remarkable center minimum. Since the temperature is highest at the center of the discharge tube and falls towards the wall of the tube, the temperature correction tends to reduce the center minimum.

Using the temperature profile shown in Fig. 15 we obtained the ion-density variation as shown in Fig. 20. The center minimum is still quite clear. In order to further establish the existence of the minimum, we used an extreme temperature model in which the temperature at the wall was assumed to be at room temperature. This model gives the maximum temperature variation across the tube and thus minimizes the center minimum. The ion-density variation based on this temperature model is shown in Fig. 21; the center minimum is still clearly seen.

The absolute number density of ArH^+ ions at the center of the tube was calculated using the results given in Fig. 12 and the temperatures given in Fig. 18, as a function of discharge current for various pressures. The results are shown in Fig. 22. We note that contrary to the line intensities given in Fig. 12, the ion density for the pressure of 1 Torr is approximately proportional to the discharge current. The large difference between the low-pressure case (1 Torr) and the higher-pressure case (3–10 Torr) mentioned earlier is even amplified in Fig. 22 because of the higher temperatures for the lower-pressure discharge given in Fig. 15.

VI. DISCUSSION

The clear cut definitive result which emerges from our observation and analysis is the marked deviation of ion-density profile from the Schottky form, especially the lo-

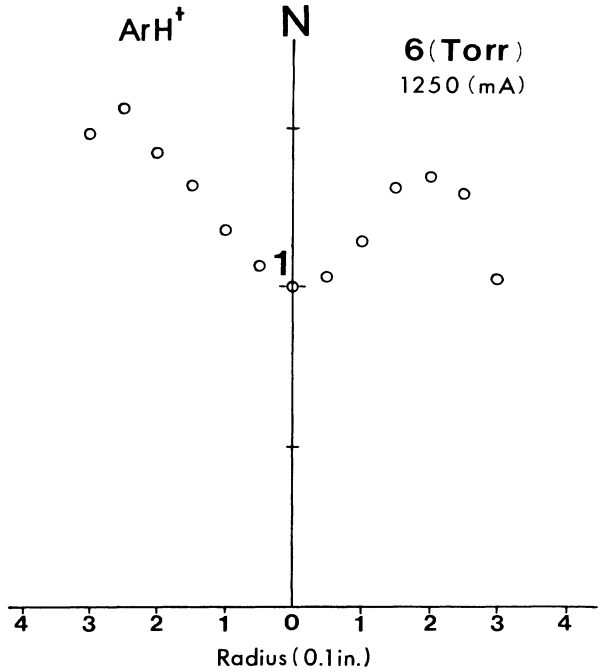

FIG. 20. The ion number density profile of ArH^+ after the temperature correction. The 6 Torr and 1250 mA data in Fig. 4 was used as the intensity profile. Here the deviation from the Schottky form is clearly seen also on the ion-density profile.

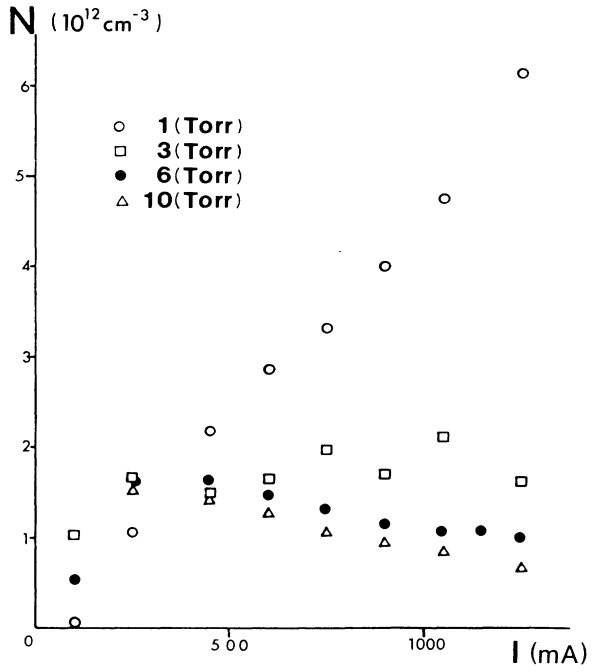

FIG. 22. The ArH^+ ion density as a function of discharge current. The raw data shown in Fig. 12 were temperature corrected using the data given in Fig. 17. The characteristic difference between the low-pressure (1 Torr) discharge and the high-pressure discharges is even more clearly seen.

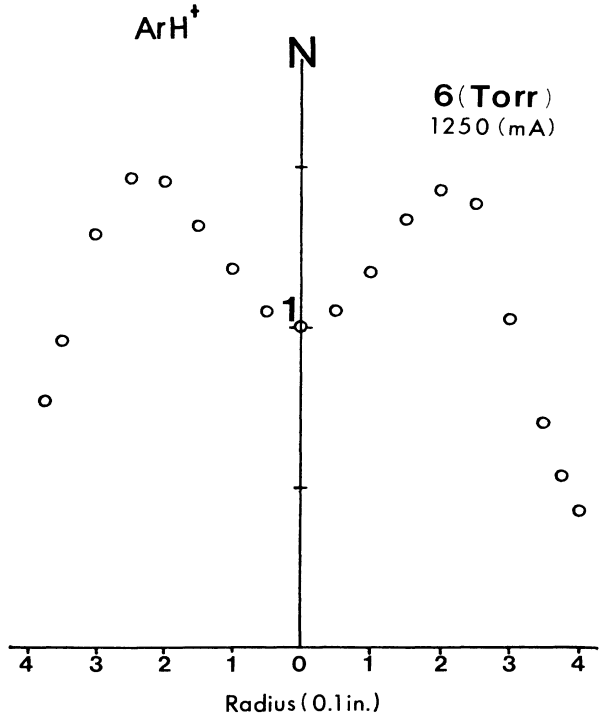

FIG. 21. The same procedure to derive Fig. 20 was repeated with the assumption of an extreme temperature variation. The clear center minimum still observable in this picture established the presence of center depletion effect (see text for details).

cal minimum at the center of discharge for high pressure-current conditions given in Figs. 4, 5, 8, 20, and 21. Such behavior has been reported for the distribution of neutral atoms in the positive column[30,31] but our results give the ion-density distributions directly. We do not have a definite explanation of this effect but in this section we try to follow previous theories in the light of our observation.

Schottky's theory[6] is based on the simplest model of ambipolar diffusion. The equation of motion for the ion-pair number density $n(r)$ as a function of the radial position r is

$$D_a \nabla^2 n(r) + \alpha n(r) = 0 \ . \tag{15}$$

In Eq. (15), α is the production rate of ion pair through single-step ionization by electron and Da is the ambipolar diffusion constant

$$D_a = \frac{D_- \mu_+ + D_+ \mu_-}{\mu_+ + \mu_-} \sim \frac{kT_e}{e} \mu_+ \ , \tag{16}$$

where T_e is the temperature of electrons, D and μ are diffusion constant and mobility, respectively, and the subscripts $+$ and $-$ refer to the positive and negative charge, respectively. The approximation in Eq. (16) results from Einstein's relation $D = \mu kT/e$ and $D- >> D+$. Using the cylindrical symmetry of the positive column, Eq. (15) is rewritten as

$$D_a \frac{1}{r} \frac{d}{dr} \left[r \frac{dn(r)}{dr} \right] + \alpha n(r) = 0 \ , \tag{17}$$

which has the solution of $J_0(\sqrt{\alpha/D}\,r)$. In using Eqs. (15) and (17), it is assumed that (a) the only production mechanism of ion pairs is by single-step ionization by electrons (which have the same number density as the ion pair), (b) the only destruction mechanism is the wall loss by ambipolar diffusion, and (c) the temperature is constant across the tube.

In 1964, Ecker and Zoller published a theoretical paper in which they relinquished the third assumption mentioned above and took into account the radial dependence of temperature. The ambipolar diffusion is then determined by the pressure gradient rather than by the density gradient. Replacing dn/dr by $(1/kT)dP/dr$ with $P=nKT$, they obtained

$$D_a \frac{1}{r}\frac{d}{dr}\left[r\left[\frac{dn(r)}{dr}+\frac{n}{T}\frac{dT(r)}{dr}\right]\right]+\alpha n=0\ . \qquad (18)$$

Solving this equation numerically, they obtained radial distribution curves which deviate from the Schottky form as shown in Fig. 23. Their results show higher ion density to the wall and, in the extreme case, some small minimum at the center of the tube. Their curves in this case resemble our results of ArH^+ in He and H_3^+ shown in Figs. 10 and 11, respectively. However, their calculation does not predict the sharp minimum we observed at the center of the discharge. This may be due to the smaller thermal conductivity and hence larger temperature gradient in the ArH^+-Ar discharges.

Oskam suggested that the center depletion observed in this paper is due to the radial cataphoresis earlier reported in the positive column of a Cs-Ar discharge by Bleekrode and Tongeren[30,31] using atomic spectroscopy of Cs. If so, this will be the first direct evidence on the distortion of ion-density distribution due to cataphoresis. While rigorous mathematical treatment of the effect is beyond the scope of the paper, we will attempt in what follows to check the possibility of this interpretation using a crude, order-of-magnitude estimation.

The radial cataphoresis is due to the fast ambipolar diffusion which depletes the ingredient in the discharge by transporting it to the wall of the discharge tube. In our case, this corresponds to the depletion of the H_2 molecule density in the center of the discharge. The discharge mixture which showed the most pronounced center depletion was Ar:H_2 of 10 Torr:30 mTorr. Thus the number density of H_2 is $\sim 10^{15}$ cm^{-3}. The steady-state number density of ArH^+ is 10^{12} cm^{-3} (based on our observation), and the fast ambipolar diffusion velocity is ~ 30 m/sec; this shows that about 3×10^{16} cm^3/sec of H_2 is depleted in the center region. This estimate of ambipolar diffusion velocity is based on the recent remarkable observation of Ganguly and Garscadden[32] that the radial ambipolar diffusion velocity is comparable to the ion axial drift velocity. The axial drift velocity of ArH^+ is estimated from the dc discharge electric field of 5 V/cm and the mobility of Ar^+ in Ar of 1.2×10^3 cm/sec per V/cm. Since our experiment is done in a flowing gas tube, the supply of fresh H_2 is on the order of 10^{17} cm^2/sec. Thus the depletion due to ambipolar diffusion seems to be a sizable portion of H_2. There is, however, two qualitative differences between the Cs atom and H_2 molecule. Firstly, for Cs atom, the neutralization of the Cs^+ ion immediately supplies the Cs atom at the wall which produces the dramatic accumulation of Cs atoms near the wall. In the case of ArH^+, however, the electron recombination

$$ArH^+ + e^- \rightarrow Ar + H \qquad (19)$$

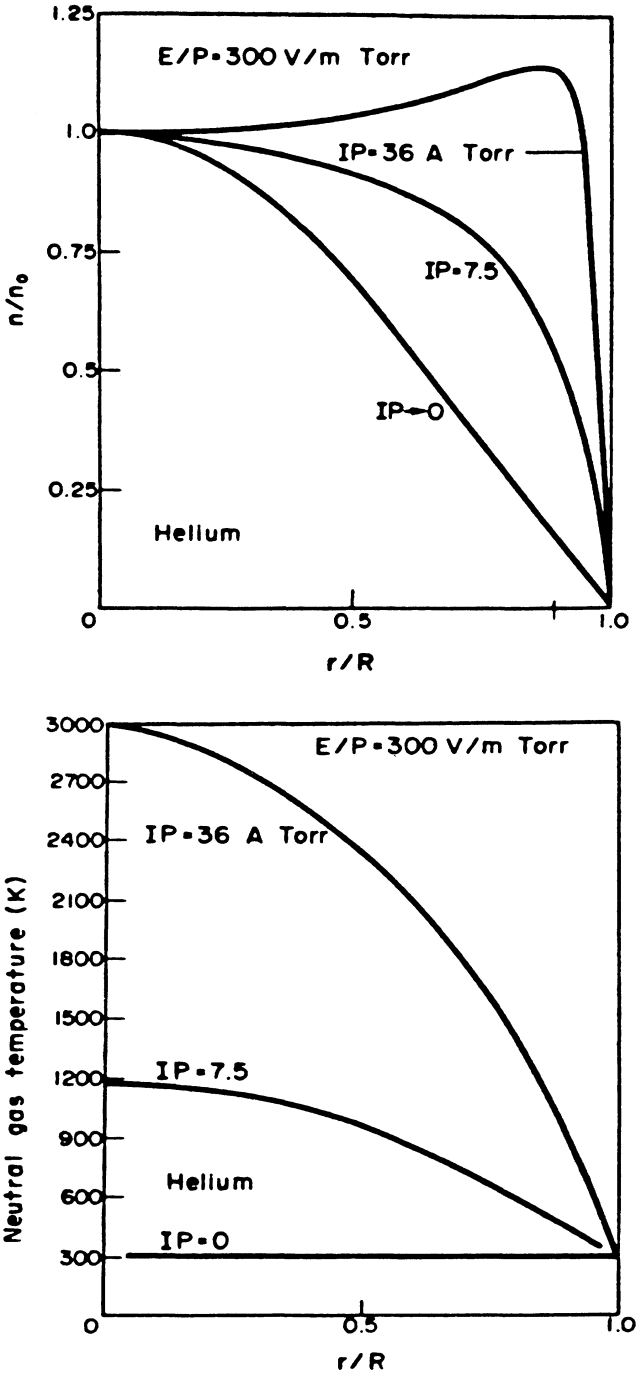

FIG. 23. Ion number density and the temperature profiles across the positive column from pure He discharge theoretically calculated by Ecker and Zoller (Ref. 10) (see text for detail).

at the wall produces Ar and H atoms. The H atom does not produce H_2 because the associative reaction $H + H \rightarrow H_2$ is extremely slow. The reaction $H + H^+ \rightarrow H_2^+$ following the ionization is also slow. Thus, unlike the case of Cs, the H_2 depleted from the center of the discharge tube is not regenerated at the wall. Secondly, the diffusion of H_2 to the depleted region is very much faster than that of Cs because of the large difference in mass. If only pure diffusion occurs, this process is still slow compared to the ambipolar diffusion, but the turbulence would make the process much faster. This may be the reason that our center depletion of the ArH^+ ion is not as complete as in the case of Cs atom. The absence of center depletion for our H_3^+ result (Fig. 11) is in agreement with this interpretation because H_2 is the only ingredient of the discharge. The other experimental result, however, contradicts this interpretation of our result as due to cataphoresis. The ArH^+ ion in the He discharge has a much higher mobility[5] and thus a higher ambipolar diffusion velocity. This would make the depletion of H_2 in the center of the discharge tube more complete, which is contrary to our observation in Fig. 10.

ACKNOWLEDGMENT

We would like to thank H. J. Oskam for suggesting cataphoresis as the possible mechanism for the observed center depletion and for valuable discussions. This work is supported by National Science Foundation Grant No. PHYS-84-08316.

[1]S. C. Brown, in *Gaseous Electronics,* edited by M. N. Hirsch and H. J. Oskam (Academic, New York, 1978), Vol. II, p. 1.
[2]*Electric Breakdown and Discharges in Gases,* edited by E. E. Kunhardt and L. H. Luessen (Plenum, New York, 1983).
[3]C. S. Gudeman and R. J. Saykally, Ann. Rev. Phys. Chem. **35**, 387 (1984).
[4]T. J. Sears, J. Chem. Soc. Faraday Trans. 2 **83**, 111 (1987).
[5]N. N. Haese, F. Pan, and T. Oka, Phys. Rev. Lett. **50**, 1575 (1983).
[6]W. Schottky, Z. Phys. **25**, 342, 635 (1924).
[7]B. E. Cherington, *Gaseous Electronics and Gas Lasers* (Pergamon, New York, 1979).
[8]E. Spenke, Z. Phys. **127**, 221 (1950).
[9]A. V. Eletskii and B. M. Smirnov, Zh. Tekh. Fiz. **40**, 1682 (1970) [Sov. Phys.—Tech. Phys. **15**, 1308 (1971)].
[10]G. Ecker and O. Zoller, Phys. Fluids **7**, 1996 (1964).
[11]W. Lindinger, Phys. Rev. A **1**, 238 (1973).
[12]G. Francis, in *The Glow Discharge at Low Pressure,* Vol. 22 of *Handbuch der Physik,* edited by S. Flugge (Springer-Verlag, Heidelberg, 1956).
[13]T. Oka, Phys. Rev. Lett. **45**, 531 (1980).
[14]J. M. Brault and S. P. Davis, Phys. Scr. **25**, 268 (1982).
[15]R. A. Gottcho and T. A. Miller, Pure Appl. Chem. **56**, 189 (1984).
[16]C. S. Gudeman, C. C. Martner, and R. J. Saykally, Chem.
[17]F. Pan, W. A. Kreiner and T. Oka (unpublished).
[18]T. Oka, *Molecular Ions: Spectroscopy, Structure and Chemistry,* edited by T. A. Miller and V. E. Bondybey (North-Holland, Amsterdam, 1983).
[19]D. Smith and N. G. Adams, Astrophys. J. **284**, L13 (1984).
[20]R. Johnsen, C. Huang, and M. A. Biondi, J. Chem. Phys. **65**, 1539 (1976).
[21]G. D. Carney and R. N. Porter, J. Chem. Phys. **60**, 4251 (1974); **65**, 3547 (1976).
[22]P. Rosmus, Theoret. Chim. Acta **51**, 359 (1979).
[23]R. Bleekrode and J. W. v. d. Laarse, J. Appl. Phys. **40**, 2041 (1969).
[24]A. von Engle, *Ionized Gases* (Oxford University Press, New York, 1965).
[25]T. Oka, Philos. Trans. R. Soc. London Ser. A **303**, 543 (1981).
[26]J. K. G. Watson, S. C. Foster, A. R. W. McKellar, P. Bernath, T. Amano, F. Pan, M. W. Crofton, R. S. Altman, and T. Oka, Can. J. Phys. **62**, 1875 (1984).
[27]D. W. Ernie and H. J. Oskam (private communication).
[28]C. H. Townes and A. L. Schawlow, *Microwave Spectroscopy* (McGraw-Hill, New York, 1955).
[29]D. J. Liu, W. Ho, and T. Oka, J. Chim. Phys. (to be published).
[30]R. Bleekrode, J. Appl. Phys. **38**, 5062 (1967).
[31]R. Bleekrode and H. von Tangeren, J. Appl. Phys. **44**, 1941 (1973).
[32]B. N. Ganguly and A. Garscadden, Phys. Rev. A **32**, 2544 (1985).